Mem. S.A.It. Suppl. Vol. 11, 124

Memorie della
Supplementi

Analysis of impact craters on Mercury's surface

E. Martellato[1], G. Cremonese[1], F. Marzari[2], M. Massironi[3], M.T. Capria[4]

(1) INAF – Osservatorio Astronomico, Vic. Osservatorio 5, I-35122 Padova, Italy
(2) Dipartimento di Fisica, Università di Padova, Padova, Italy
(3) Dipartimento di Geologia, Università di Padova, Padova, Italy
(4) INAF – IASF, Roma

Abstract. The formation of a crater is a complex process, which can be analyzed with numerical simulations and/or observational methods. This work reports a preliminary analysis of some craters on Mercury, based on the Mariner 10 images. The physical and dynamical properties of the projectile may not derive from the knowledge of the crater alone, since the size of an impact crater depends on many parameters. We have calculated the diameter of the projectile using the scaling law of Schmidt and Housen (, 1987). It is performed for different projectile compositions and impact velocities, assuming an anorthositic composition of the surface. The melt volume production at the initial phases of the crater formation is also calculated by the experimental law proposed by O'Keefe and Ahrens (, 1982), giving the ratio between melt and projectile mass.

Key words. Planets: individual: Mercury; Planets: geology

1. Introduction

The study of impact craters began with the observation of the Moon by Galileo Galilei. However, only at the end of 19th century, an impact origin for these observed circular cavities was proposed by Gilbert considering only vertical impacts. This hypothesis was not accepted by the astronomers because the vertical impacts are extremely unlikely in planetary events. Indeed, the probability that a meteoroid of an isotropic flux hits a planetary surface with an inclination between ϑ and $\vartheta + d\vartheta$ is:

$$dP = 2 \sin\vartheta \cos\vartheta d\vartheta \qquad (1)$$

The probability is thus zero for vertical or grazing impact, i.e. 90^o and 0^o respectively, while it gets the maximum value at 45^o (Gault & Wedekind (, 1978)).

The analysis of impact craters has a great importance in many aspects of research:

1) to analyze the flux of impacting objects in the Inner Solar System about 3.9 Gy ago;
2) to date the geologic units;
3) to study the atmosphere formation;
4) to understand the crustal and upper lithospheric structure of planets.

Indeed, the discontinuities in planetary crust may affect the impact crater formation. The presence of faults in the superficial layer affects both the crater shape and the ejecta distribution. For example, the Meteor Crater (Arizona) exhibits a square shape instead of a circular one. A vertical layering affects both the crater and the ejecta morphology. The

Send offprint requests to: E.Martellato: elena.martellato@oapd.inaf.it

case of a weaker and incoherent layer over a stronger and more compact one may lead to the formation of a concentric crater, if the impact energy is high enough. This property is taken to quantify the depth of the regolith layer in the Moon. On the other hand, the presence of a permafrost layer at depth is invoked to explain the peculiar ejecta blanket around martian rampart craters. Indeed, an enough energetic projectile may get the ice layer, so as to support the debris fluidization.

2. Crater Morphology

In this study we analyze some Mercury impact craters, which represent one of the most important and frequent feature that characterize its surface. All the fresh craters are characterized by a near-circular raised rim, a floor deeper than the crater surroundings, and an ejecta blanket around the crater itself. The crater morphology is size-dependent as follows:

- *Simple craters*: $D < 10km$. They are bowl-shaped cavities, with a depth-diameter ratio of about 1/5. When the crater diameter exceeds a critical value, depending of planet gravity, the crater morphology undergoes a deep transformation.
- *Complex craters*: $10km < D < 100km$. They are cavities characterized by the presence of central peaks, terraced walls and flat floor, with a depth of about 2-4 km (Cintala & Head (, 1976)). The central peaks are composed by rocks above the pre-impact surface, that uplifted about 8% of the crater diameter.
- *Multi-ring basins*: $D > 750km$. They are composed by several rings, that are neither circular, nor concentric, while their center is filled by dark basaltic floods. An example is the Caloris Basin, the youngest and largest one (about 1300 km in diameter) known so far.

3. Impact Process

The formation of an impact crater is a process characterized by the transfer of the initial energy of a projectile from itself to the target surface, in order to originate a ”hole”. We can identify the three following phases:

- *Contact and compression*; begins when the projectile strikes the target surface, that is pushed, compressed and accelerated. At the same time the projectile is decelerated due to the resistance to penetration of the target. During this process, the kinetic energy of the projectile is converted into internal energy of both projectile and target, giving rise to a shock wave that propagates in both materials. When both materials unload from the compressed state, they may undergo phase transformations, such as melting or vaporization.
- *Excavation and growth* of the transient crater; that is characterized by two major processes, that are the expansion and decay of the shock wave and the opening of the cavity crater by the excavation flow. As the shock wave travels across the target: 1) it engulfs more material but weakens, degrading to a stress wave; 2) it sets target material into motion, radially away from the impact site immediately behind the shock wave. Rarefaction waves create an upward-directed pressure gradient behind the shock, adding an upward component to the radial velocity, initiating the excavation flow, in which the main mass of material is ejected from the crater. The excavation flux enlarges the cavity, that has been opened during the previous stage, until, at the end of this stage, it assumes a hemispherical shape. At this point of the process, the crater diameter is said *transient crater*.
- *Modification*; the transient crater is modified by gravity in more stable structures, depending upon the size of the crater, the gravitational field of the planet, and the yield of the surface and sub-surface rocks. The simple craters do not undergo important alteration, but the slumping of the crater walls into the floor. Instead, the complex craters exhibit an entirely different structure from the bowl shaped transient crater: wide scale collapse and elastic rebound processes cause the uplift of the

rocks underlying the crater's center (central peaks and rings) and the formation of terraces along the crater walls.

4. Data analysis

The aim of this study is to analyze some Mercury craters in order to calculate the *diameter L* of the impactor and the *melt volume* produced during the first phase of the impact process. We have selected some complex craters in the diameter range of 50-100 km and Tab.1 reports the list.

Impact cratering is a complex process, since it depends on many parameters. So, it is described by assuming some simplifying hypothesis, which may reproduce the impact event with more or less accuracy:

1) the projectile is spherical;
2) the target has an homogeneous composition;
3) the impact is vertical

The first assumption is realistic, because the shock wave travels in a hemispherical way, if the impact velocity is enough high, independent from the projectile shape. The second represents a simplified, but reliable, case of the more general one (i.e. layered and faulted surface). As just pointed out, the last assumption is not consistent with the flux models of impactors towards a planetary surface (Strom et al. (, 2005)).

4.1. The projectile diameter

Understanding the characteristics of the projectile which has originated a given crater is not univocal, since the final crater dimensions depend on many parameters, such as the projectile physical and dynamic properties and the planet properties. The theoretical, experimental and numerical approaches led to the formulation of an equation, named *scaling law*, which establishes the functional dependence of the impact outcome on the problem parameters. It is based on the assumption that the kinetic energy of the projectile affects the outcome, irrespective of its separate size and velocity. So, it is introduced a single-dimensional parameter, the *coupling parameter*, the value of which affects on one's own the final crater. In this case, the scaling relationships assume the form of *power laws*, which represent a comparison between dimensionless combinations of quantities describing the projectile and the final crater. The proportional constants and the exponents depend on the impactor and target material, and are obtained by experiments(Holsapple (, 1993), Holsapple et al. , 2002), Melosh (, 1989), Richardson et al. (, 2005), Schultz et al. (, 2005)). In this work we use the scaling law of Schimdt and Housen (, 1987)):

$$L = 0.828(\frac{\rho_{pr}}{\rho_t})^{-0.42} D_{sc}^{0.20} D^{1.09} * \\ * g^{0.28} v_i^{-0.56} \qquad (2)$$

which allows us to calculate the projectile diameter L, once known the impact velocity v_i, the final crater diameter D, projectile and target composition, ρ_{pr} and ρ_t respectively, the simple-to-complex transition diameter D_{sc}, which depends on the planet gravitation field, and finally the gravity g. The projectile diameter L has been calculated assuming different values for its density and impact velocity, as summarized in Tab. 2, while we considered anorthosite for the Mercury's surface with $\rho_t = 2.734 g/cm^3$.
The results of the analysis are reported in Tab. 3, where the crater diameter, in the second column, has been measured by ourselves.
In Fig. 1 and Fig 2, we report two examples of Mercury craters, Degas and March respectively, with a very different ejecta patterns we can encounter on Mercury surface. In the first one, we can observe that impact has *not* been vertical with respect to planetary surface, because rays show an asymmetrical pattern. By analyzing Degas ejecta pattern, we can infer that the impact angle is ranged in 20^o and 45^o. So, the calculated diameter value is preliminary, because we had to take into account the effects of the impact angle in Eq. 2. Nevertheless, this analysis could not been

Table 1. List of the analysed Mercury craters. The content of each column is the following: name of the crater; latitude and longitude; diameter; spatial resolution in the Mariner 10 images.

Crater	Coordinates	Diameter (km)	Resolution (km/px)
Ajvaghosa	10.4N, 21.0W	90	0.67
Balzac	10.3N, 144.1W	80	0.92
Brahms	58.5N, 176.2W	96	0.22
Degas	37.4N, 126.4W	60	1.44
Kuiper	11.3N, 31.1W	62	1.16
March	31.1N, 175.5W	70	0.98
Martial	69.1N, 177.1W	51	0.25
Repin	19.2N, 63.0W	107	0.78

applied to all Mercury craters, because most of the craters do not have a clear ejecta deposit, as in the case of March (Fig. 2). This is caused by the fact that Mercury has a greater gravity than the Moon, and the fragments travel for a lower distance from principal crater during the excavation phase (Strom & Sprague (, 2003). So, a higher image resolution is requested to detect the ejecta layer. Another reason is given by the fact that the ejecta blanket can be masked by subsequent impacts.

4.2. The melt volume

Melting takes place during a planetary impact event when material is decompressed from the high-pressure state, originated by the travelling shock wave. Shock compression is represented by Hugoniot equations, which express the conservation laws of mass, momentum, and energy. A dimensional comparison between these three equations, which linked pressure, energy and velocity, shows a dependence of the ratio between melt and projectile mass from the impact velocity (Melosh (, 1989), Pierazzo & Vickery (, 1997), Pierazzo & Melosh (, 2000)). To calculate melt volume we adopted the equation of O'Keefe and Ahrens (, 1982):

$$\frac{Mass of Melt}{Mass of projectile} = 0.14\frac{v_i^2}{\varepsilon_m} \quad (3)$$

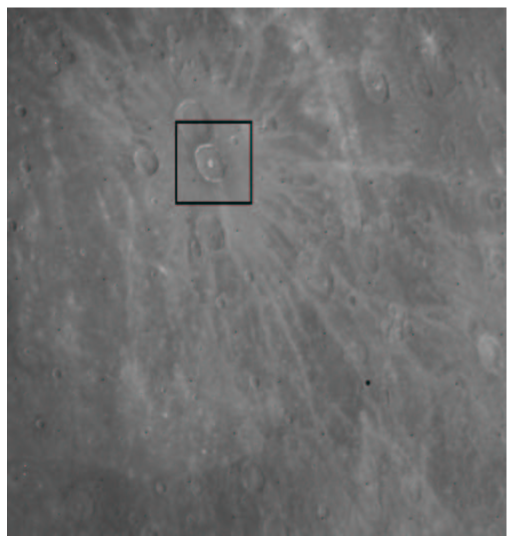

Fig. 1. Mariner 10 image of the crater Degas (37.4N, 126.4W), that exhibits a rayed ejecta blanket.

where ε_m is the specific internal melting energy of the target material. We observe that this equation has as lower limit v_i=12 km/s. Results are reported in Tab. 4.

The impact angle affects considerably also the melt production, which decreases with increasing obliquity. As reported in Pierazzo & Melosh (, 2000), the melt volume can drop below one-half of the vertical impact, if the impact angle is lower than 30^o.

Table 2. Input parameters for impactor, ρ and v_i.

		Density g/cm^3	Velocity km/s
meteoroids	Iron	7.8	34
	Chondrite	3.58	34
Comets	Parabolic	0.4	87
	Periodic	0.4	44

Table 3. Results of our analysis, reporting the projectile diameter for different compositions.

Craters	Measured Diameter (km)	Projectile Diameter (km) Iron Meteoroids	Chondrite Meteoroids	Parabolic Comets	Periodic Comets
Ajvaghosa	92 ± 6	4 ± 0.3	5 ± 0.4	8 ± 0.5	11 ± 0.8
Balzac	80 ± 2	3 ± 0.1	4 ± 0.1	7 ± 0.2	10 ± 0.3
Brahms	95.5 ± 4.5	3.9 ± 0.20	5.5 ± 0.28	8.1 ± 0.41	11.9 ± 0.61
Degas	61 ± 2	2 ± 0.1	3 ± 0.1	5 ± 0.2	7 ± 0.3
Kuiper	62 ± 5	2 ± 0.2	3 ± 0.3	5 ± 0.4	7 ± 0.6
March	70 ± 4	3 ± 0.2	3.9 ± 0.2	6 ± 0.3	8 ± 0.5
Martial	51.5 ± 5.6	2.0 ± 0.24	2.8 ± 0.33	4.1 ± 0.49	6.1 ± 0.72
Repin	107 ± 4	4 ± 0.2	6 ± 0.3	9 ± 0.4	13 ± 0.5

Table 4. Results: Melt volume.

Craters	Measured Diameter (km)	Melt Volume (10^{12} m^3) Iron Meteoroids	Chondrite Meteoroids	Parabolic Comets	Periodic Comets
Ajvaghosa	92 ± 6	30 ± 6.5	37 ± 8.0	89 ± 19.0	72 ± 15.3
Balzac	80 ± 2	19 ± 1.6	24 ± 1.9	56 ± 4.7	45 ± 3.7
Brahms	95.5 ± 4.5	35.0 ± 5.34	42.8 ± 6.54	102.3 ± 15.62	82.2 ± 12.56
Degas	61 ± 2	8 ± 0.9	10 ± 1.1	24 ± 2.5	19 ± 2.0
Kuiper	62 ± 5	9 ± 2.1	11 ± 2.6	25 ± 6.2	20 ± 4.9
March	70 ± 4	13 ± 2.3	16 ± 2.8	38 ± 6.7	30 ± 5.4
Martial	51.5 ± 5.6	4.6 ± 1.65	5.7 ± 2.02	13.5 ± 4.84	10.9 ± 3.89
Repin	107 ± 4	51 ± 6.3	63 ± 7.7	150 ± 18.5	121 ± 14.9

5. Future Work

Future work will consist in improving our comprehension of crater morphology, allowing a better testing of the 3D performances of Stereo imaging Channel (STC), in the SIMBIOSYS instrument, in the BepiColombo

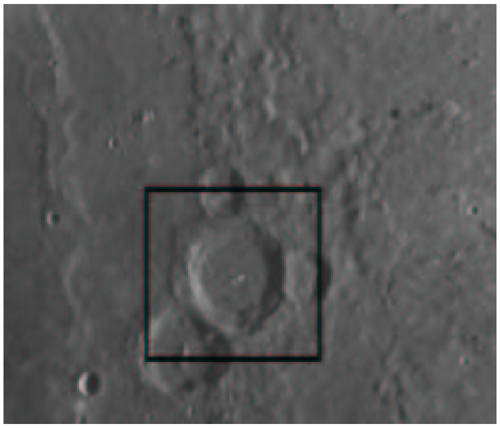

Fig. 2. Mariner 10 image of the crater March (31.1N, 175.5W).

mission Da Deppo et al. (, 2006). The STC may provide the information required to the comprehension of the process which gives origin to an impact crater and to a better knowledge of Mercury surface history.

Moreover, the reconstruction 3D of craters allows us to test a new method, proposed by Wallis et al. (, 2005), to determine the azimuthal impact direction and the impact angle. The authors assumed that the topographic crater profile $z(r, \vartheta)$ may be expressed as a linear combination of eigenfunctions $\phi_m n(r, \vartheta)$:

$$z(r, \vartheta) = \sum_{n=1}^{N} \sum_{m=1}^{M} c_{mn} \phi_{mn}(r, \vartheta) \quad (4)$$

The expansion of coefficients c_{mn} allows to isolate the radially symmetric and asymmetric components of the crater, because both symmetric and asymmetric functions are present in Eq. 4, and it provides both impact direction and angle.

References

Cintala, M.J., & Grieve, R.A.F. 1998, Meteoritics & Planetary Science, 33, 889

Cintala, M.J., Head, J.H., & Mutch, T.A. 1976, in: Proc. Lunar Sci. Conf. 7th, 3575

Gault, D.E., & Wedekind, J.A. 1978, in: Proc. Lunar Sci. Conf. 9th, 3843

Da Deppo, V., Naletto, G., Cremonese, G., Debei, S., & Flamini, E. 2006, in: Proc. of the SPIE, 6265

Holsapple, K.A. 1993, Annu. Rev. Earth Planet. Sci., 21, 333

Holsapple, K.A. et al. 2002, in: Asteroids III, eds. W. Bottke et al., The University Arizona Press, Tucson, 443

Melosh, H.J. 1989, Impact cratering: a geologic process, Oxford Univ. Press, New York

O'Keefe, J.D., & Ahrens, T.J. 1982, J. Geophys. Res., 87, 6668

Pierazzo, E., & Melosh, H.J. 2000, Icarus, 145, 252

Pierazzo, E., Vickery, A.M., & Melosh, H.J. 1997, Icarus, 127, 408

Richardson, J.E., Melosh, H.J., Artemieva, N.A., & Pierazzo, E. 2005, Space Sci. Rev., 117, 241

Schmidt, R.M., & Housen, K.R. 1987, Int. J. Impact Engin., 5, 543

Schultz, P.H., Ernst, C.M., & Anderson, J.L.B. 2005, Space Sci. Rev., 117, 207

Strom, R.G., & Sprague, A.L. 2003, Exploring Mercury, the iron planet, Springer Praxis Publishing, Chichester, UK

Strom, R.G., Malhotra, R., Yoshida, F., & Kring, D.A. 2005, Science, 309, 1847

Wallis, D., Burchell M.J., Cook, A.C., Solomon, C.J., & McBridge 2005, MNRAS, 359, 1137